Energy budget analyses of scenario earthquake ruptures at Cascadia

Betsy Madden, elizabeth.madden@sjsu.edu

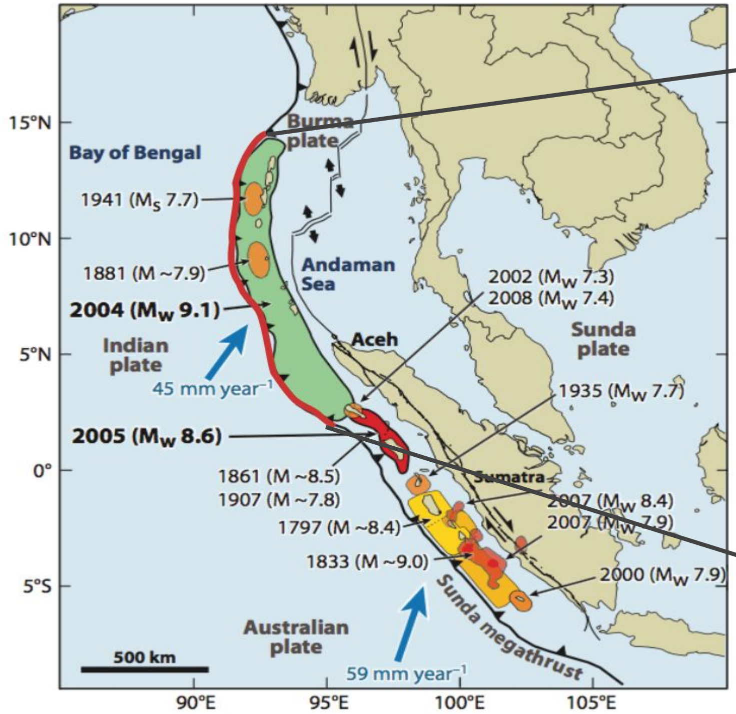

Shearer & Burgmann (2010)

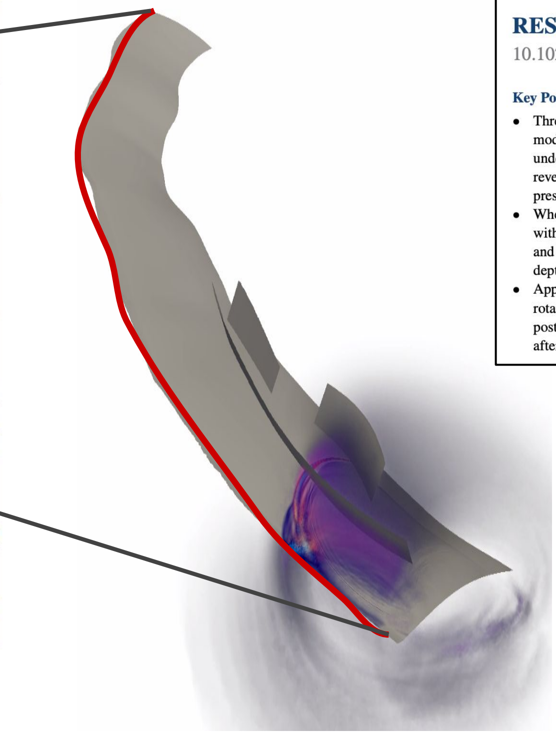

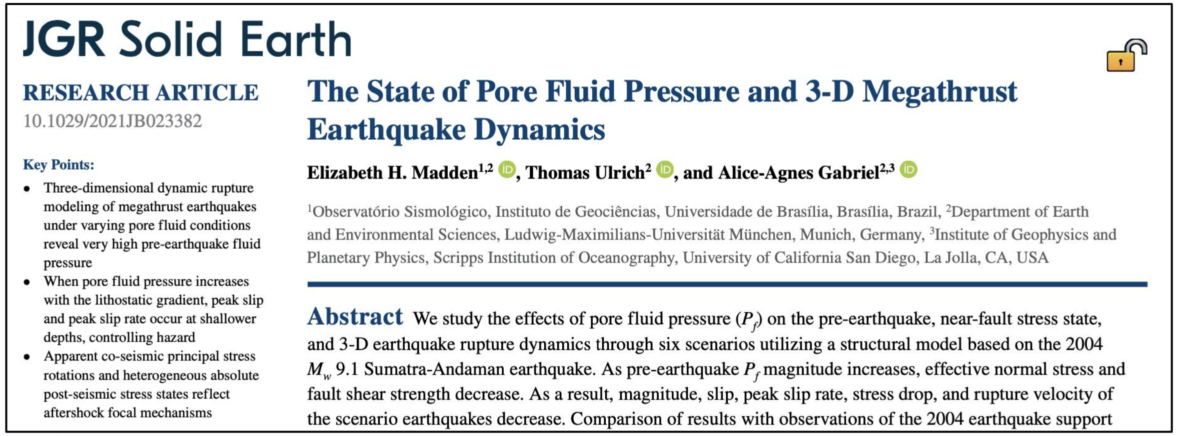

JGR Solid Earth

RESEARCH ARTICLE

10.1029/2021JB023382

The State of Pore Fluid Pressure and 3-D Megathrust Earthquake Dynamics

Elizabeth H. Madden[1,2], Thomas Ulrich[2], and Alice-Agnes Gabriel[2,3]

[1]Observatório Sismológico, Instituto de Geociências, Universidade de Brasília, Brasília, Brazil, [2]Department of Earth and Environmental Sciences, Ludwig-Maximilians-Universität München, Munich, Germany, [3]Institute of Geophysics and Planetary Physics, Scripps Institution of Oceanography, University of California San Diego, La Jolla, CA, USA

Key Points:

- Three-dimensional dynamic rupture modeling of megathrust earthquakes under varying pore fluid conditions reveal very high pre-earthquake fluid pressure
- When pore fluid pressure increases with the lithostatic gradient, peak slip and peak slip rate occur at shallower depths, controlling hazard
- Apparent co-seismic principal stress rotations and heterogeneous absolute post-seismic stress states reflect aftershock focal mechanisms

Abstract We study the effects of pore fluid pressure (P_f) on the pre-earthquake, near-fault stress state, and 3-D earthquake rupture dynamics through six scenarios utilizing a structural model based on the 2004 M_w 9.1 Sumatra-Andaman earthquake. As pre-earthquake P_f magnitude increases, effective normal stress and fault shear strength decrease. As a result, magnitude, slip, peak slip rate, stress drop, and rupture velocity of the scenario earthquakes decrease. Comparison of results with observations of the 2004 earthquake support

LMU LUDWIG-MAXIMILIANS-UNIVERSITÄT MÜNCHEN

VolkswagenStiftung

Universidade de Brasília

Lindsay Gross (Twinning Mentee 2024-25)
Sean Hsieh (MS, Computer Science)
Corey Liscombe (SJSU Undergraduate Research Opportunity Program)

SJSU SAN JOSÉ STATE UNIVERSITY

CRESCENT CASCADIA REGION EARTHQUAKE SCIENCE CENTER

Geoscience Education and Inclusion
UNDERGRADUATE TWINNING PROGRAM

4 models with high or very high co-seismic pore fluid pressure (Pf) and lithostatic or sub-lithostatic Pf gradient

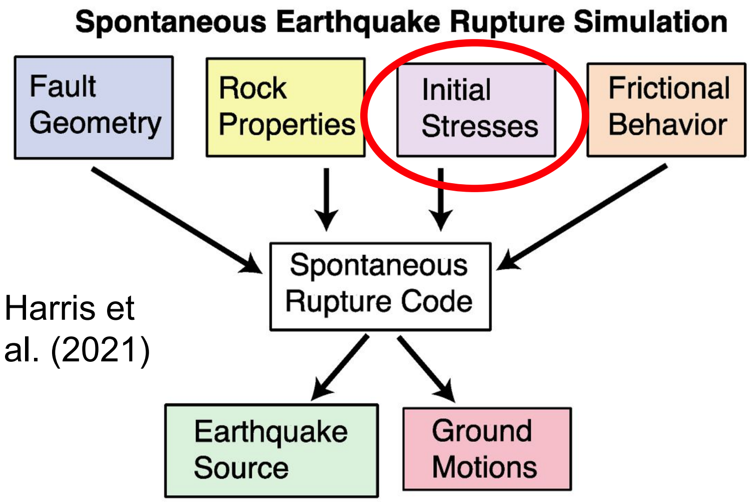
Spontaneous Earthquake Rupture Simulation

Fault Geometry

Rock Properties

Initial Stresses

Frictional Behavior

Spontaneous Rupture Code

Earthquake Source

Ground Motions

Harris et al. (2021)

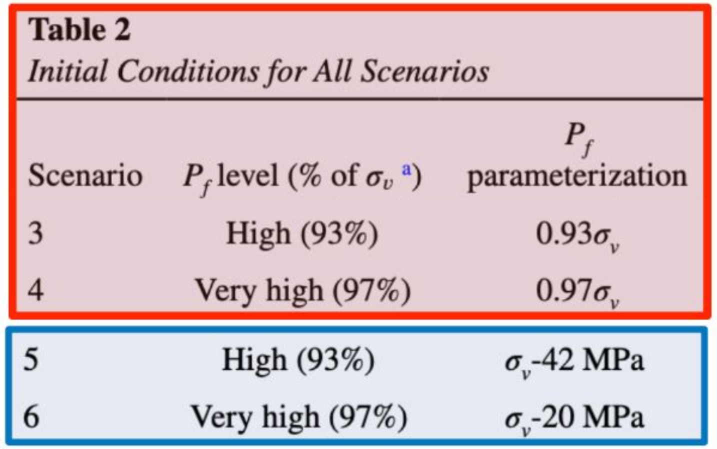
Table 2

Initial Conditions for All Scenarios

Scenario	P_f level (% of σ_v [a])	P_f parameterization
3	High (93%)	$0.93\sigma_v$
4	Very high (97%)	$0.97\sigma_v$
5	High (93%)	σ_v-42 MPa
6	Very high (97%)	σ_v-20 MPa

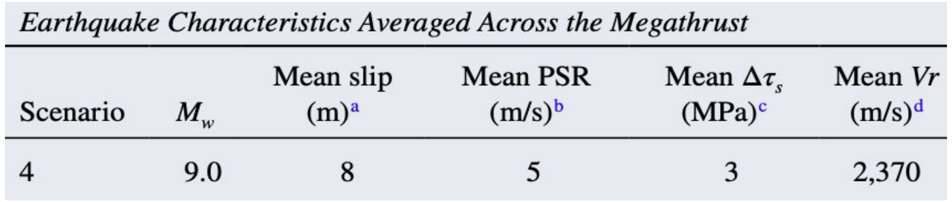
Earthquake Characteristics Averaged Across the Megathrust

Scenario	M_w	Mean slip (m)[a]	Mean PSR (m/s)[b]	Mean $\Delta\tau_s$ (MPa)[c]	Mean Vr (m/s)[d]
4	9.0	8	5	3	2,370

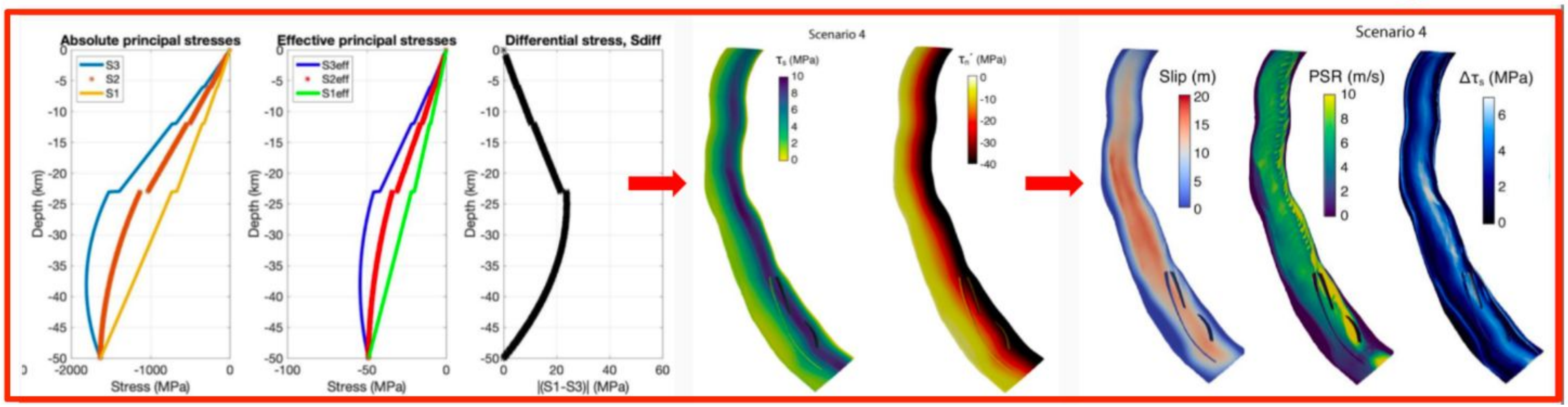

4 models with high or very high co-seismic pore fluid pressure (Pf) and lithostatic or sub-lithostatic Pf gradient

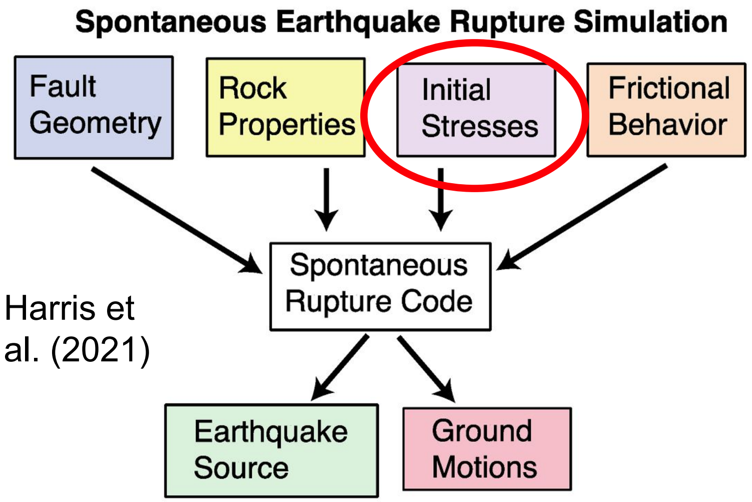

Spontaneous Earthquake Rupture Simulation

Fault Geometry

Rock Properties

Initial Stresses

Frictional Behavior

Spontaneous Rupture Code

Earthquake Source

Ground Motions

Harris et al. (2021)

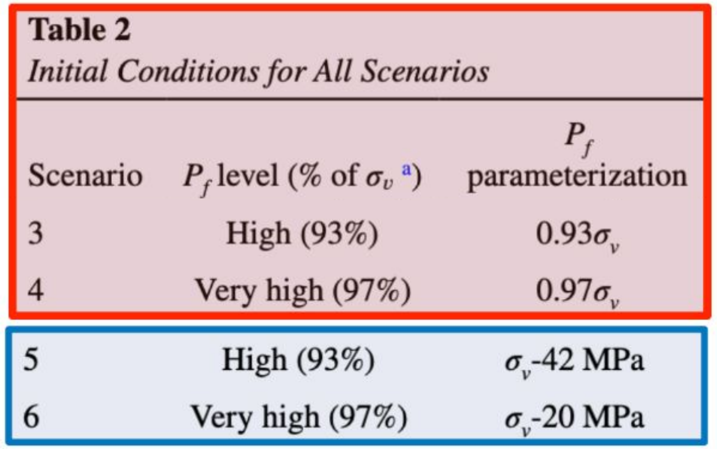

Table 2

Initial Conditions for All Scenarios

Scenario	P_f level (% of σ_v [a])	P_f parameterization
3	High (93%)	$0.93\sigma_v$
4	Very high (97%)	$0.97\sigma_v$
5	High (93%)	σ_v-42 MPa
6	Very high (97%)	σ_v-20 MPa

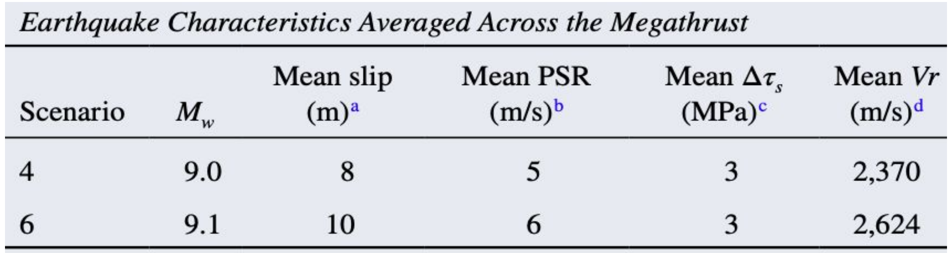

Earthquake Characteristics Averaged Across the Megathrust

Scenario	M_w	Mean slip (m)[a]	Mean PSR (m/s)[b]	Mean $\Delta\tau_s$ (MPa)[c]	Mean Vr (m/s)[d]
4	9.0	8	5	3	2,370
6	9.1	10	6	3	2,624

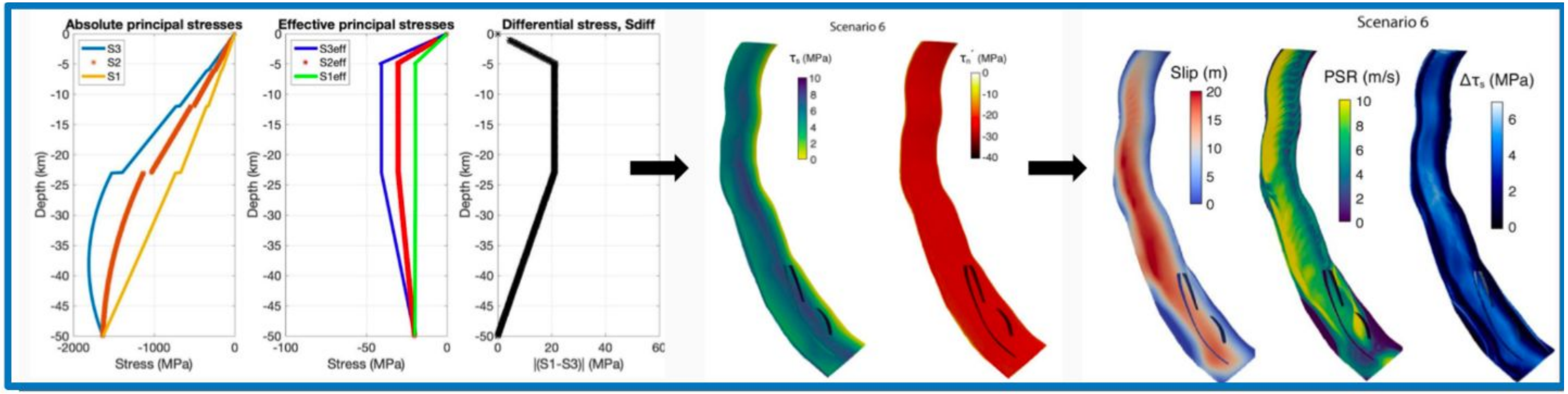

Earthquake energy budget

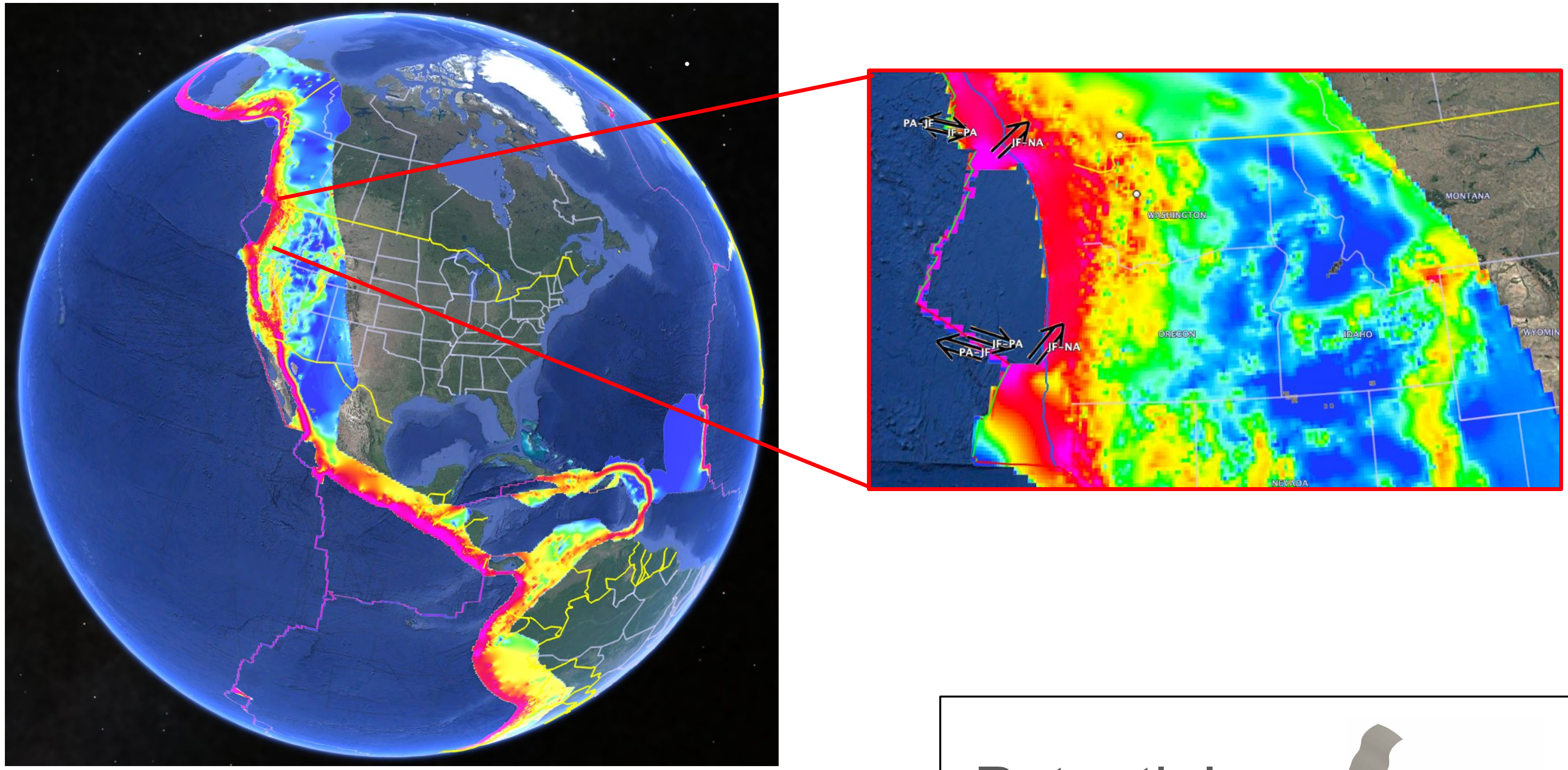

Global crustal strain rate model from horizontal geodetic data (v.2.1) (Kreemer et al., 2014)

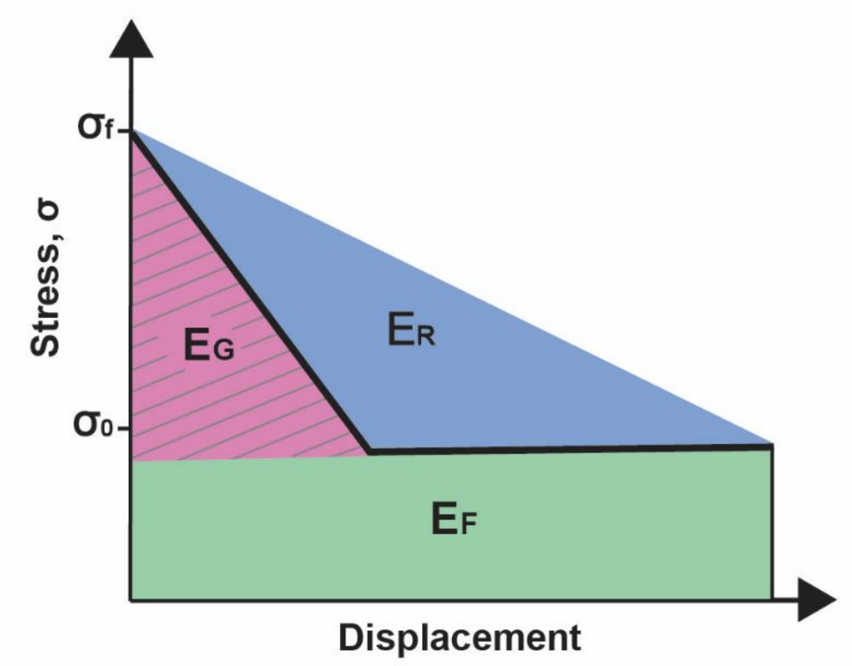

(Coffey et al., 2023)

Potential strain energy

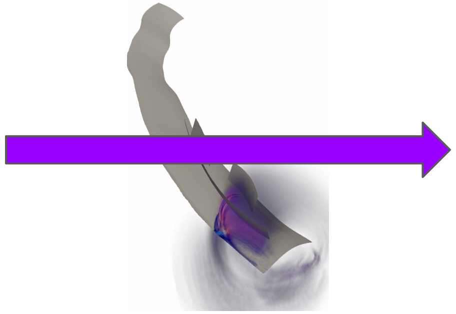

EG: fracture energy
EF: frictional energy
ER: radiated energy

Earthquake energy budget

$$W_{\text{total}} = \int_{\Sigma} \boldsymbol{\sigma}_0(\boldsymbol{\xi}) \cdot \boldsymbol{\Delta u}_1(\boldsymbol{\xi}) d\Sigma - \int_0^{\infty} \int_{\Sigma} \boldsymbol{\sigma}(\boldsymbol{\xi}, t) \cdot \boldsymbol{\Delta v}(\boldsymbol{\xi}, t) d\Sigma dt$$

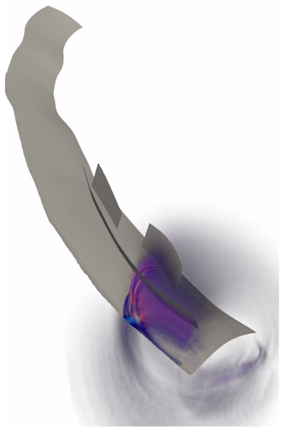

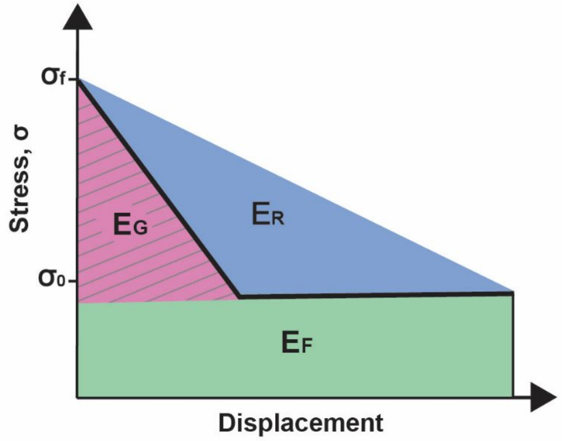

(Coffey et al., 2023)

EG: fracture energy
EF: frictional energy

$$W_{\text{static}} = \frac{1}{2} \int_{\Sigma} [\boldsymbol{\sigma}_0(\boldsymbol{\xi}) - \boldsymbol{\sigma}_1(\boldsymbol{\xi})] \cdot \boldsymbol{\Delta u}_1(\boldsymbol{\xi}) d\Sigma$$

ER: radiated energy

$$E_R = W_{\text{total}} - W_{\text{static}} = \int_{\Sigma} \frac{\boldsymbol{\sigma}_0(\boldsymbol{\xi}) + \boldsymbol{\sigma}_1(\boldsymbol{\xi})}{2} \cdot \boldsymbol{\Delta u}_1(\boldsymbol{\xi}) d\Sigma - \int_0^{\infty} \int_{\Sigma} \boldsymbol{\sigma}(\boldsymbol{\xi}, t) \cdot \boldsymbol{\Delta v}(\boldsymbol{\xi}, t) d\Sigma dt.$$

W = work
Σ = fault surface
Δu_1 = final slip
Δv = slip velocity
t = time
σ_0 = initial shear stress
σ = shear stress
σ_1 = final shear stress

Ma & Archuleta (2006)

Energy budgets for 2004 Sumatra earthquake models

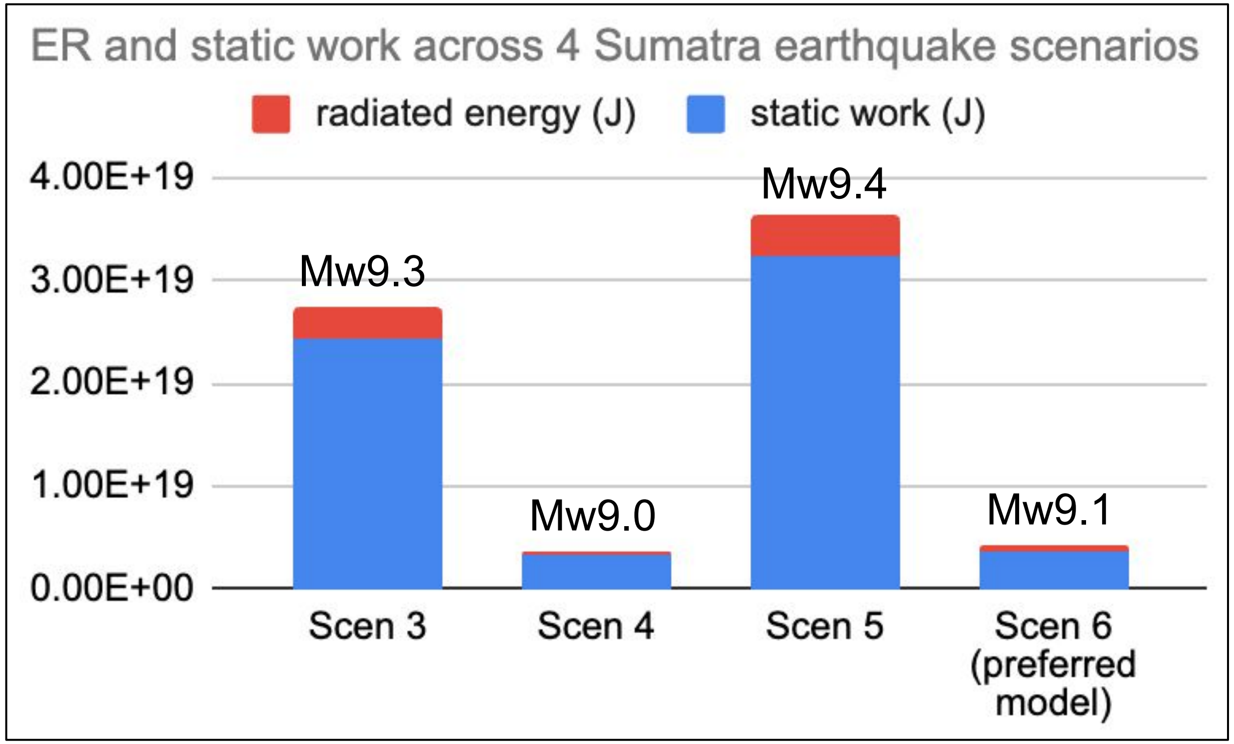

- Total energy scales with magnitude

Energy budgets for 2004 Sumatra earthquake models

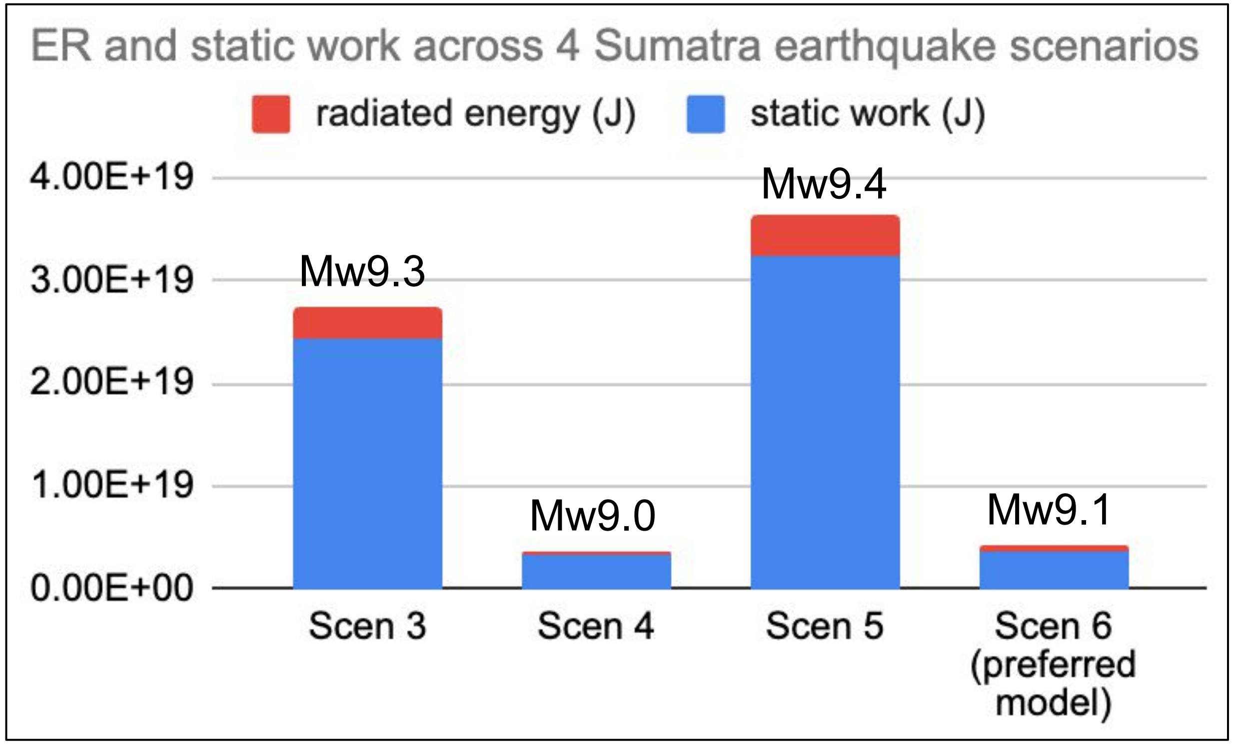

- Total energy scales with magnitude

- All 4 earthquake models have the same energy budget

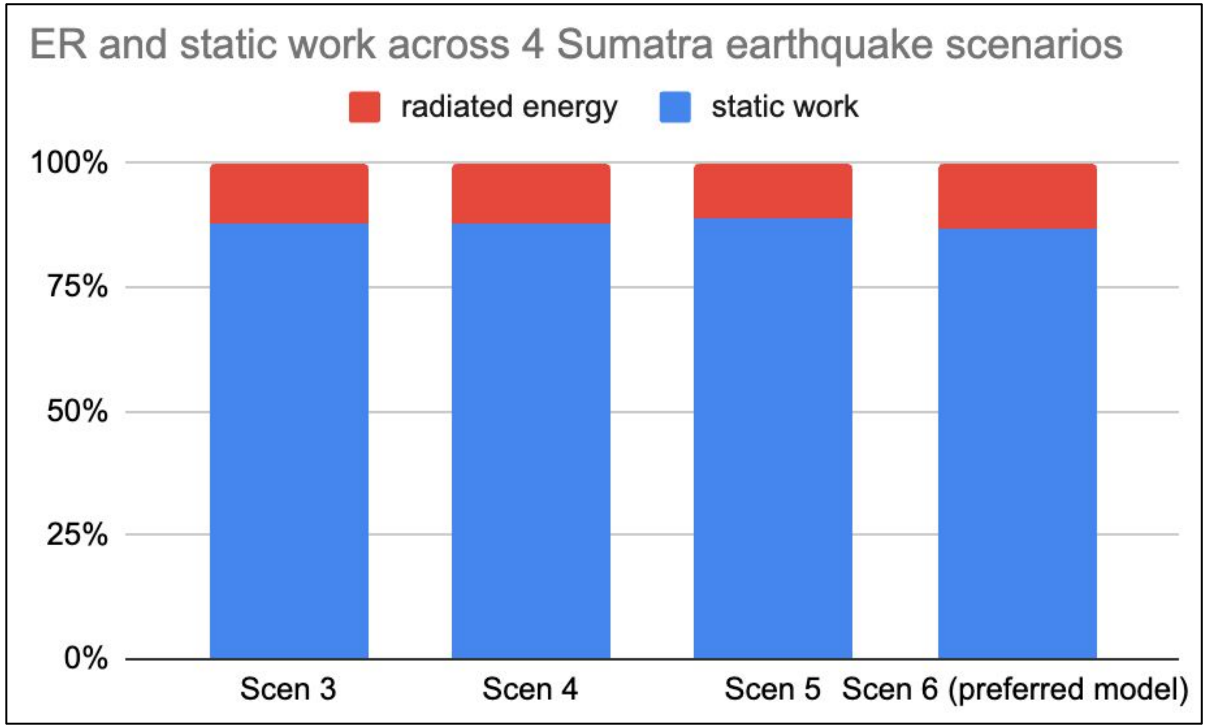

Energy budget for 2004 Sumatra earthquake

- Models match ER in order of magnitude, but are almost twice as high
- High ER results in low ER/M0

Energy Component	**Observations** (Kanamori, 2006, Table 1)	**Model - Sumatra Scenario 6**
Mw	9.1	9.1
Seismic Moment (M0)	**6.5 E+22 J**	4.93 E+22 J
Total Work (Wt)	n/a	4.23 E+18 J
Static Work (Ws)	n/a	3.67 E+18 J
ER = Wt-Ws	3 E+17 J	**5.60 E+17 J**
ER/M0	4.6 E-6	**1.14 E-05**

Cascadia scenario earthquake ruptures & energy budgets

	Observations - Sumatra	Model - Sumatra	Model - Cascadia
Mw	9.1	9.1	
Seismic Moment (M0)	**6.5 E+22 J**	4.93 E+22 J	
Total Work (Wt)	n/a	4.23 E+18 J	
Static Work (Ws)	n/a	3.67 E+18 J	
ER = Wt-Ws	3 E+17 J	**5.60 E+17 J**	
ER/M0	4.6 E-6	**1.14 E-05**	

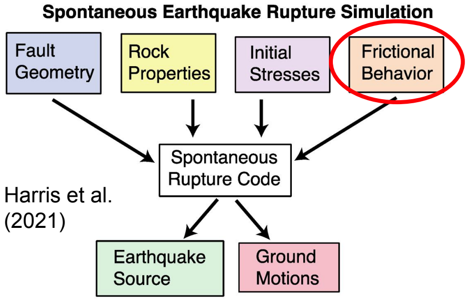

Spontaneous Earthquake Rupture Simulation

Fault Geometry

Rock Properties

Initial Stresses

Frictional Behavior

Spontaneous Rupture Code

Earthquake Source

Ground Motions

Harris et al. (2021)

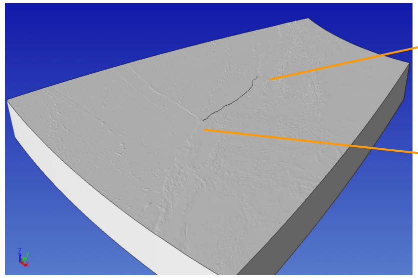

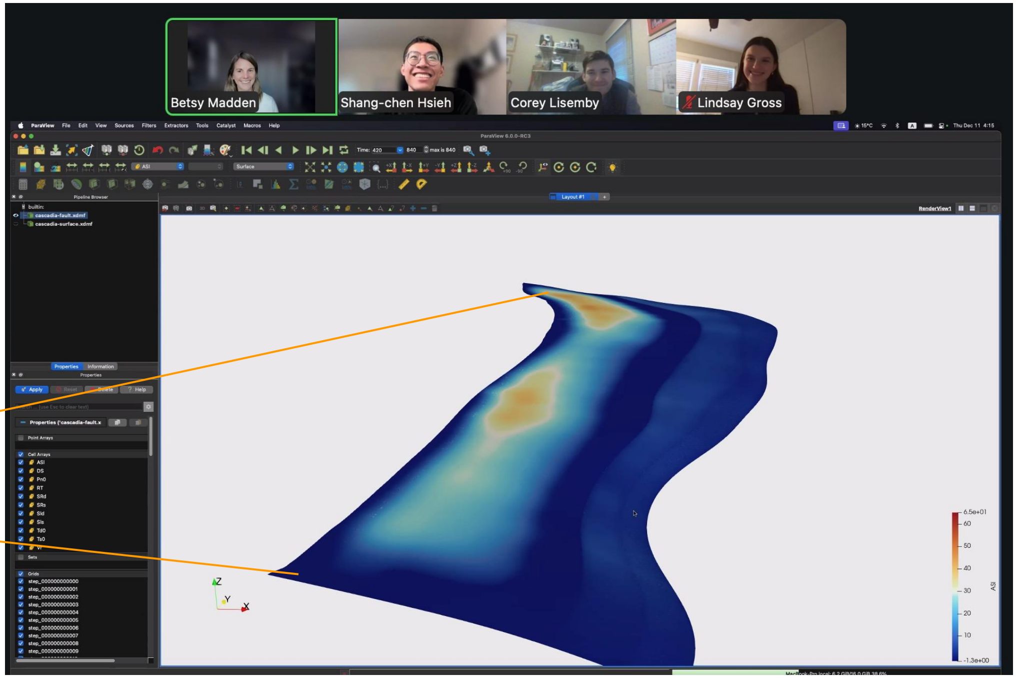

Let σ_{ij} denote the stress tensor. Define:

Mean stress $\sigma_m = \frac{1}{3}(\sigma_{11} + \sigma_{22} + \sigma_{33})$

Stress deviator $s_{ij} = \sigma_{ij} - \sigma_m \delta_{ij}$

Second invariant of the stress deviator $J_2(\sigma) = \frac{1}{2}\sum_{i,j} s_{ij} s_{ji}$

Drucker-Prager yield stress $Y(\sigma) = \max(0,\ c\cos\phi - (\sigma_m + P_f)\sin\phi)$

Drucker-Prager yield function $F(\sigma) = \sqrt{J_2(\sigma)} - Y(\sigma)$

The Drucker-Prager material is required to satisfy the *yield equation*: $F(\sigma) \le 0$

When $F(\sigma) < 0$, the material behaves like a linear elastic material, with Lame parameters λ and μ.

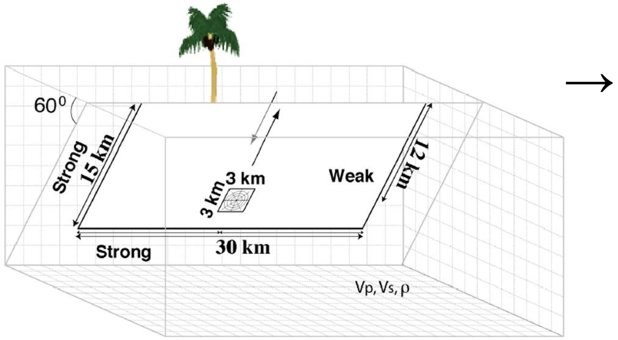

Harris et al. (2018)

→ Add off-fault plasticity

→ Evaluate different megathrust interface geometries Elston et al. (2025)